Fractal and topological properties of directed fractures

G. Caldarelli,[1] C. Castellano,[2,3] and A. Vespignani[2]

[1]*Scuola Internazionale Superiore di Studi Avanzati, via Beirut 2-4, I-34014 Grignano di Trieste, Italy*
[2]*Dipartimento di Fisica, Università di Roma "La Sapienza," Piazzale Aldo Moro 2, I-00185 Roma, Italy*
[3]*Dipartimento di Scienze Fisiche, Università di Napoli, Mostra d'Oltremare, Padiglione 19, I-80125 Napoli, Italy*
(Received 13 September 1993)

We use the Born model for the energy of elastic networks to simulate "directed" fracture growth. We define directed fractures as crack patterns showing a preferential evolution direction imposed by the type of stress and boundary conditions applied. This type of fracture allows a more realistic description of some kinds of experimental cracks and presents several advantages in order to distinguish between the various growth regimes. By choosing this growth geometry it is also possible to use without ambiguity the box-counting method to obtain the fractal dimension for different subsets of the patterns and for a wide range of the internal parameters of the model. We find a continuous dependence of the fractal dimension of the whole patterns and of their backbones on the ratio between the central- and noncentral-force contributions. For the chemical distance we find a one-dimensional behavior independent of the relevant parameters, which seems to be a common feature for fractal growth processes.

PACS number(s): 64.60.Ak, 62.20.Mk, 05.40.+j

I. INTRODUCTION

There is a great variety of solid cracks in nature over a wide range of length scales showing a rich phenomenology and very different physical processes ranging from cleavage to ductile fracture [1,2]. Recently, a large number of studies has been devoted to these processes from the point of view of statistical mechanics and pattern formation. In order to characterize the properties of fracture patterns, a wide variety of models based on deterministic or probabilistic growth processes has been introduced [1–3]. In particular, the underlying fractal properties of paths leads to the definition of several models of fracture propagation. The inspiration comes from the study of nonequilibrium fractal growth processes, such as the dielectric breakdown model [4] and diffusion limited aggregation [5]. However, due to the high complexity of the fracture propagation problem, it is very difficult to obtain large crack growth simulations [6].

Two very interesting models are the central-force model [7] and the improved model due to Yan, Li, and Sander [8], where noncentral forces are introduced by using the Born model [9,10] for the elastic energy. This model is the analogy for fracture propagation of the dielectric breakdown model for Laplacian growth, describing very simply the fracture propagation controlled by growth instabilities (probabilistic mechanism). Moreover, this model allows one to take into account the vectorial nature of the problem. The numerical simulations show that the patterns are fractal with an exponent depending on the parameter of the model [8]. In addition, several variations of the model with different local growth rules were investigated [11].

In general numerical simulations of this model are mainly focused on patterns presenting circular symmetry. However, there are several kinds of real crack phenomena showing an anisotropic behavior. For instance, two-dimensional cuts through stress corrosion cracks in alloys show connected fracture patterns which propagate along crystallographic planes known as cleavage planes [12] and present a well-defined growth direction. For this type of fractures the fractal dimension is better estimated with covering methods and the usual mass-gyration radius relation is not well defined [12]. In addition, different growth geometries affect the value of the fractal dimension, so that the results obtained with simulations in circular geometry are not directly comparable with several real fracture phenomena. This last point is relevant also from a theoretical point of view such as, for instance, in the fixed scale transformation (FST) method [13,14] that refers better to cylindrical geometry for a comparison of the analytical results.

Here we present computer simulations of fractures generated using the Born model with uniaxial tension. We obtain crack patterns showing a preferential evolution direction, which we define as "directed" fractures. These patterns seem to be a realistic description of cracks with a well-defined growth direction. The simulations are generated in cylindrical geometry, allowing us to work with two independent length scales (the height h and the width L) and therefore to evaluate more clearly the various scaling regimes of these structures [15]. In fact, in the cylinder geometry there are two different growth phases: a scaling regime for pattern heights smaller than the size of the basis of the lattice and a steady state which continues indefinitely afterwards [15]. In the scaling regime the patterns show a complicated self-affine behavior, while in the steady state they are statistically self-similar with well-defined asymptotic fractal properties. This growth geometry allows us also to introduce in a very simple way the concepts of chemical distance and backbone that characterize the topological and connectivity properties of the patterns. Moreover, the exponents governing the fractal scaling of these subsets provide extremely useful parameters to characterize the fractures

beyond the simple fractal dimension.

We study numerically several realizations of the Born model in two dimensions. We analyze the morphology of the patterns and we show the essential features of fractures not to be affected by variations of the kind of strain uniaxially applied or the shape of the seed. By using a box-counting method, which gives results not affected by the anisotropy of patterns, we obtain for the steady-state regime (self-similar region) the fractal behavior of the Born model for several values of its internal parameters. We can distinguish with sufficient accuracy between small changes of these parameters, obtaining different results in comparison to previous simulations [8]. In particular, the wide range of parameters investigated indicates a continuous dependence of the fractal dimensions of the cluster (D_F) and of the backbone (D_B) on the ratio between central- and noncentral-force contribution. This is in contrast with the results of Ref. [8] predicting the existence of two universality classes for the model. On the contrary, the chemical distance seems to have a fractal dimension $D_C = 1$, independently of the model parameters.

The paper is organized as follows. In Sec. II the growth model is introduced and the details for the realization of the simulations are specified. Section III is devoted to the concepts of backbone and chemical distance that provide further information on the geometrical properties of the generated clusters. In Sec. IV we report and discuss the results obtained.

II. THE MODEL

In our simulations the elastic medium is modeled by a two-dimensional network of elastic springs. The Born model represents the elastic potential energy with two terms, corresponding, respectively, to the central- and noncentral-force contribution:

$$V = \frac{1}{2} \sum_{i,j} V_{ij}$$
$$= \frac{1}{2}(\alpha - \beta) \sum_{i,j} [(\mathbf{u}_i - \mathbf{u}_j) \cdot \hat{r}_{ij}]^2 + \frac{1}{2}\beta \sum_{i,j} [\mathbf{u}_i - \mathbf{u}_j]^2 , \quad (1)$$

where $\mathbf{u}_i$ is the displacement vector of site i, $\hat{r}_{ij}$ is the unit vector between i and j, α and β are force constants, and the sum runs over nearest-neighbor sites. In this model the formation of cracks in a solid is probabilistic: it is obtained through an iterative addition of broken lattice bonds to the fracture already grown. At every step the new broken bond is chosen as follows: (1) given the crack pattern, one calculates the displacement field of the sites by minimizing the energy of the lattice, i.e., Eq. (1); (2) a new broken bond is randomly chosen among those contiguous to the crack pattern; the probability for every bond is

$$p_{ij} = \frac{V_{ij}^{\eta/2}}{\sum_{ij} V_{ij}^{\eta/2}} , \quad (2)$$

where η is a free parameter of the model; and (3) the new broken bond added to the pattern modifies the boundary

conditions for the displacement field.

The behavior of the Born model is an approximation of classical elasticity. For instance, in spite of computing the energy minimum, one can set to zero the force acting on the infinitesimal volume; in this case one obtains the Lamé equation [16], which depends on two coefficients. In the Born model the energy of the network depends on two parameters, α and β, weighting the contribution of central and noncentral forces. Because we are only interested in the energy minimum, only the ratio β/α is relevant and we can tune the value of β keeping α fixed $(\alpha = 1)$.

The model is inspired by the dielectric breakdown model (DBM), of which it is the mechanical analog. In fact, the bond breaking criterion is the same and only the field used to define the probability is different, reflecting the different physical nature of the process. For this reason, a behavior similar to the DBM one is expected with respect to the parameter η (i.e., the crack's fractal dimension changes continuously as the exponent η is changed). Instead, a new relevant parameter is introduced by the elastic equation through the ratio (β/α). The latter parameter is responsible for relevant changes in the fractal dimension of patterns generated, though its effect is not very clear from previous simulations [8]. In particular, it is not well understood if it defines two universality classes (i.e., $\beta/\alpha = 0$ or $\beta/\alpha > 0$) or a continuous range of fractal dimension.

In addition, there are many other details that have to be specified, in the basic scheme described previously, because in principle their change may affect the fractal properties [7,8,11]. For example, the relevance of the connectivity rule, which changes (in some cases drastically) the fractal dimensions of clusters, is well known. We use the rule depicted in Fig. 1: (i) given the crack pattern, we define as damaged each site where at least one broken bond starts; (ii) the bonds that may be broken at the next growth step are all those starting from damaged sites. Also the elastic springs can be arranged in different kinds of networks, such as square or triangular lattice. However, on the square lattice Eq. (1) is not appropriate for $\beta = 0$ [8]. Therefore, in the following, only triangular lattices will be considered. The aim of these choices is the comparison of our results with those of Refs. [7,8,11].

Another important element is the kind of stress to be applied. The latter influences the global shape of the fracture. We apply a uniaxial tension (i.e., displacement of only two opposite sides of the strip (Fig. 2), in order to obtain directed crack patterns orthogonal to the stress.
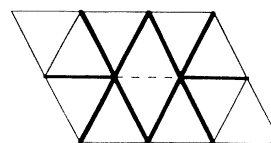

FIG. 1. The connectivity rule used in this paper: the broken bond is indicated by a dashed line. The bold lines indicate those bonds which may be broken in the next stage of growth.
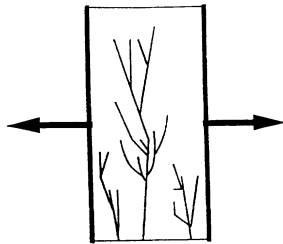
FIG. 2. Uniaxial tension applied on the medium.

With uniaxial tension it is quite natural to use fixed boundary conditions on the two sides not stressed. From the simulations we notice that two other factors are not relevant: the orientation of the lattice with respect to the stressed sides and the angle ϕ between the tension and the sides to which it is applied. In fact, a variation of these elements changes the fractal dimensions by less than 4%. Because of that, we perform our simulations with the simplest value $(\phi=0)$ for that angle.

The last detail to be specified is the shape and position of the initial seed. We perform simulations beginning with three different situations: (1) one broken bond in the middle of the strip; (2) one broken bond near one fixed boundary and perpendicular to it; and (3) one of the sides not stressed entirely made of broken bonds.

Given this set of choices the Born model depends only on the "internal" parameters α, β, and η. With these prescriptions we generate many clusters for different lattice sizes and various values of the internal parameters. The clusters generated (see Fig. 3) are very similar to DBM realizations, even if now we are dealing with a vectorial field. The reason for this behavior is the close relation between Born model and Lamé equation, which is a vectorial generalization of the Laplace equation.

III. CHARACTERIZATION OF THE FRACTAL AND TOPOLOGICAL PROPERTIES

The first quantitative description of the structures generated by our Born model is through the fractal dimen-
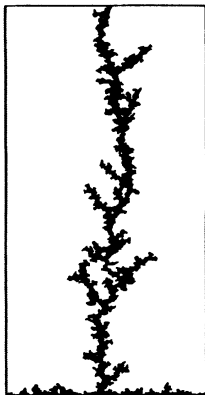

FIG. 3. A realization of a cluster with size of 128×336.

sion D_F that directly measures the scaling of density as length scale is changed. However, this parameter is not sufficient to completely characterize the clusters. Therefore it is useful to introduce some other parameters that can quantitatively describe the topological and connectivity properties of the aggregates. These parameters are the exponents governing the scaling (i.e., the fractal dimension) of two subsets of the clusters: the backbone and the chemical distance.

The latter is the shortest path between the two ends of the fracture pattern. Although this definition is topological, its physical interpretation is immediate: it is the line that really separates the elastic medium in two parts.

The backbone is generated starting from the cluster and eliminating all tips and closed loops connected to the chemical distance only by a single path (Fig. 4). Also the physical meaning of the backbone is clear: it is part of the aggregate that really changes the connectivity properties of the system affecting the macroscopic properties of the medium. For example, if we inject a liquid in the fracture, the backbone is the part of the patterns where the fluid flows.

Starting from the whole cluster there are various different algorithms to select the bonds belonging to the backbone and the chemical distance. One possible method exploits the "conductivity" properties of the subsets, giving to each broken bond a finite "random" resistance and studying, in analogy with the fluid example, the current flow in the cluster. Unfortunately some numerical problems make this method rather lengthy and not reliable. For this reason, in order to find chemical distance and backbone, we set up a computer algorithm based on the topological properties.

The shortest path between the two opposite sides of the strip is found in this way. One starts from one side (A) and follows all possible connected paths, labeling each broken bond with the distance separating it from A. In practice, this is done iteratively. At the nth step all broken bonds labeled by n are considered. Every broken nearest-neighbor bond is marked by $n+1$ unless it is already labeled (this would mean that there is a shorter path connecting it to A) (Fig. 5). When the opposite side (B) is reached, the chemical distance is identified by going backwards from B to A, i.e., passing at every step from a bond labeled by n to its nearest neighbor labeled by $n-1$.

Starting from the chemical distance, a similar process, applied several times, leads to the identification of the backbone. This subset of the aggregate is formed by the chemical distance and all closed loops connected to it by at least two nonintersecting paths. To identify these loops one starts from all nodes passed through by the chemical distance and labels every broken bond with the distance from it to the closest node and with a node label. When one finds that a nearest neighbor is already labeled, a loop is identified. But if the node label is the same, one deals with a "bad" loop as shown in Fig. 5. Only when the node label is different is the loop part of the backbone. This process must be applied several times in order to find all good loops connected to other loops and not directly to the chemical distance. In this way one has a
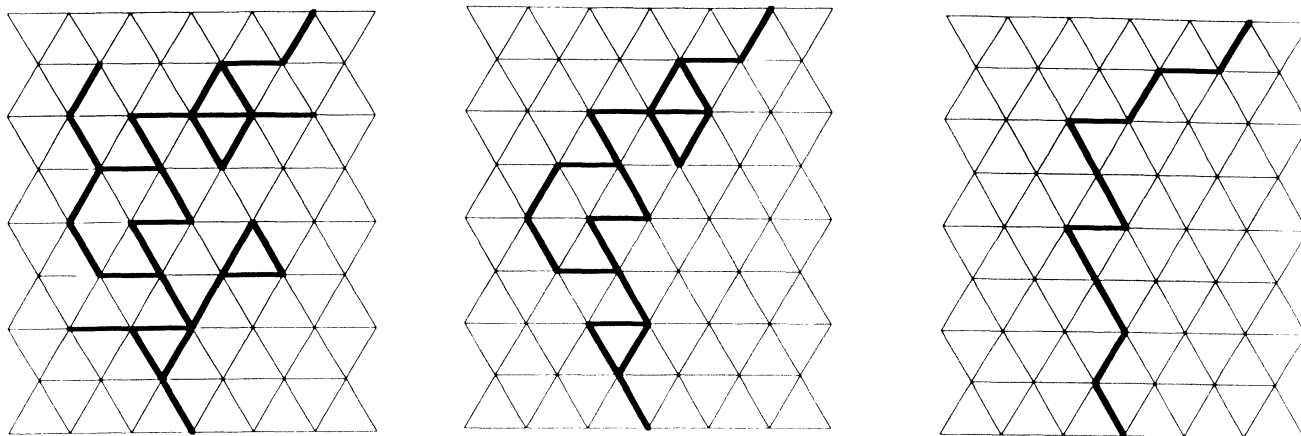
FIG. 4. The differences between the cluster (left), the backbone (middle), and the chemical distance (right) for a small aggregate.

reliable method which is even faster than the "physical" ones, because the number of steps grows as L^{D_F} instead of L^d.

It is important to note that the choice of the chemical distance is usually not unique: there are several different shortest paths leading from one side to the opposite one. We consider only one of them, because their length is the same. In this way, we can isolate from the clusters all

bonds belonging to the chemical distance or to the backbone, obtaining the corresponding substructures (Fig. 6). The fractal exponents of these subsets can be defined as the box-counting dimensions through

$$n_L(h,l) \sim l^{-D} , \tag{3}$$

where $n_L(h,l)$ is the number of $l \times l$ squares needed to cover the cluster of height h and base L, or its substruc-
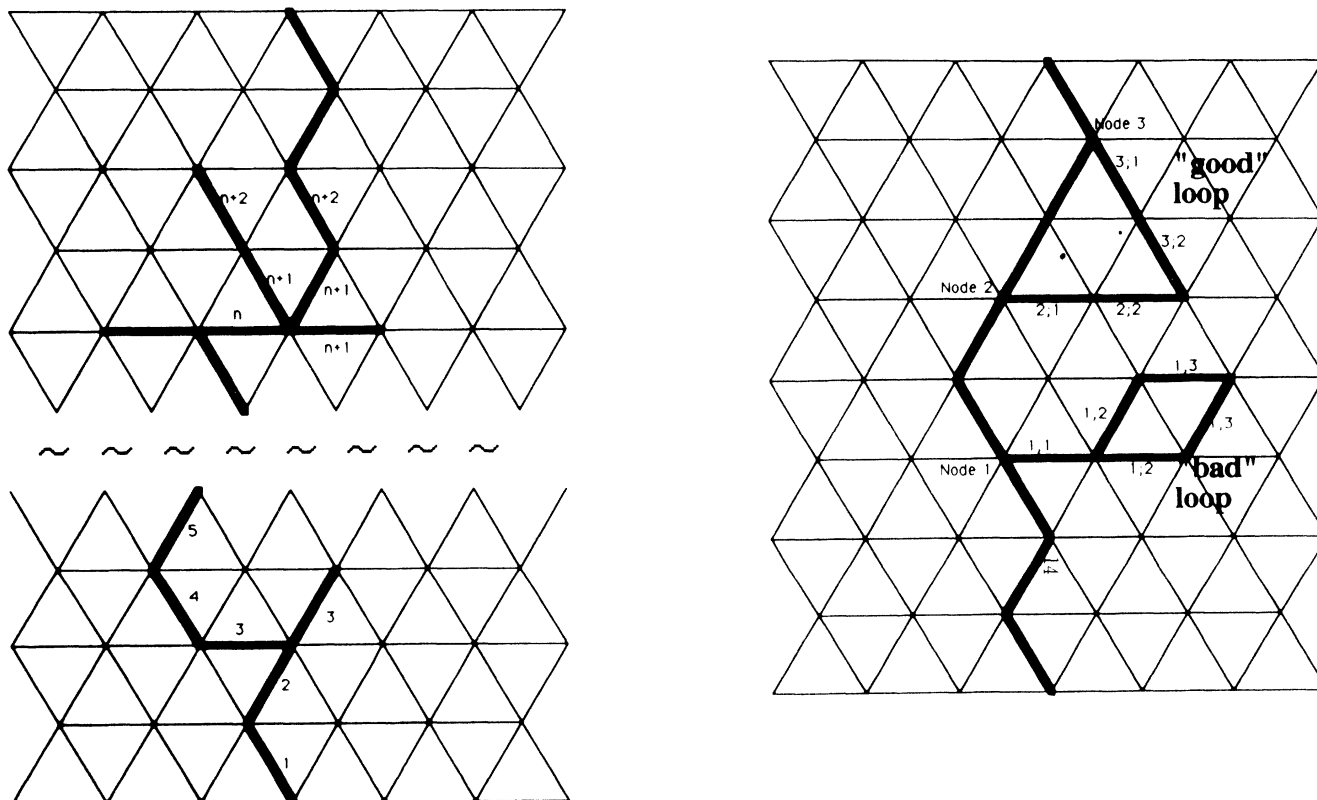

FIG. 5. Left: the labeling process for the identification of the chemical distance. Right: the identification of the backbone; the loops belonging to it are those labeled starting from two different nodes.
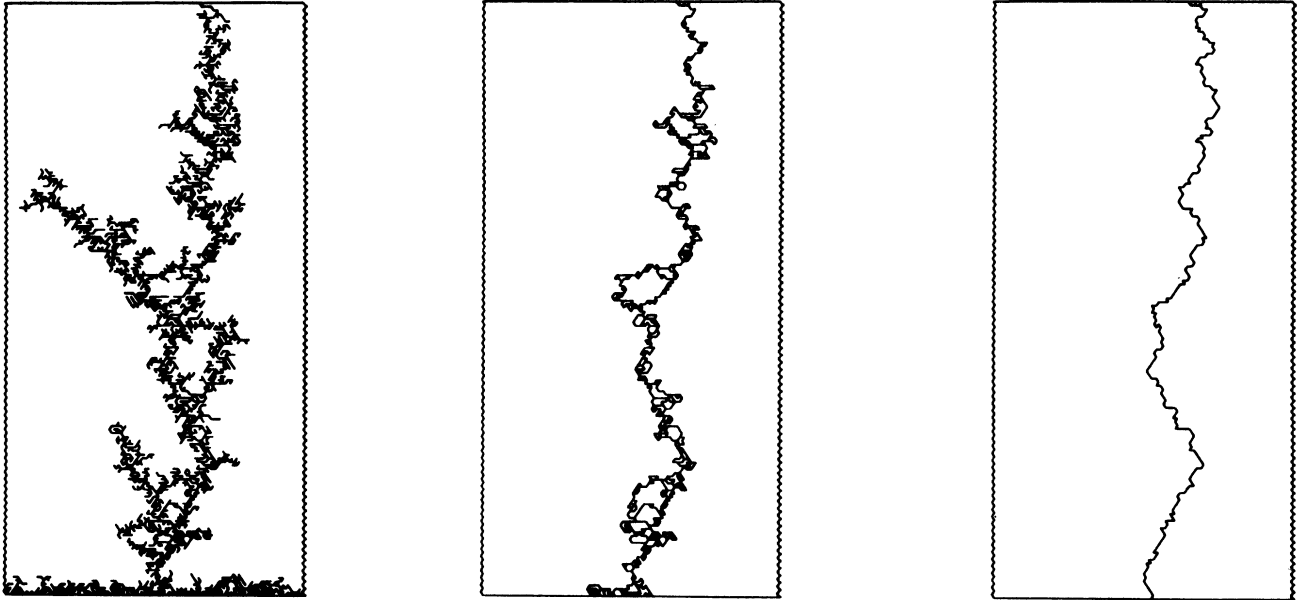
FIG. 6. The whole cluster, the backbone, and the chemical distance for a typical realization of our simulations.

tures. This equation holds for $1 \ll l \ll L$ and the exponent defined does not depend, apart from finite size effects, on h and L. This method is not affected by the anisotropy of the patterns (as the mass-radius relation) and allows us to distinguish and take into account the various growth regime and interface effects on the fractal dimension results. This is because we can analyze square sections of the patterns which are far from the boundary region of growth, eliminating the effects due to the fact that the interface has a lower fractal dimension because the structure is not asymptotically grown. In addition, we focus our analysis in a square region with height larger than the lattice basis size, in order to view only the asymptotic self-similar part of the patterns. In this way we can define without ambiguity a "frozen" steady-state region of the fractures where the scaling behavior is defined uniquely. The crack patterns are therefore characterized in this region by the three exponents D_F, D_B, and D_C, corresponding, respectively, to the fractal dimension of the whole cluster, of the backbone, and of the chemical distance.

IV. RESULTS

With the model described in the preceding section we have simulated cracks in lattices under uniaxial tension. The tension is applied on the largest sides of rectangular lattices of different sizes: 64×168 and 128×336. The clusters obtained are formed by up to 10^4 broken bonds and to our knowledge are the largest produced until now with this method. We perform eight realizations for each geometry of the seed and for each value of the internal parameters. In the following we will present the results of the simulations with three different types of seed geometry and for a wide range of values of the internal parameters.

A. Seed in the middle of the lattice

Here we show the results obtained for a seed formed by one broken bond in the middle of the rectangular lattices. A typical result for a crack pattern of this type is shown in Fig. 7. The patterns obtained are very similar to those obtained for uniaxial tension in Ref. [6]. The patterns have an elongated shape perpendicular to the applied load. There are also a high number of side branches, and the crack looks very much like a diffusion limited aggregation (DLA) cluster with anisotropic sticking probability. We observe also the instability of the crack tips, which show the tendency to split, contrary to Ref. [6]. In this sense the side branches are mainly tips that lost the competition during the tip-splitting process.

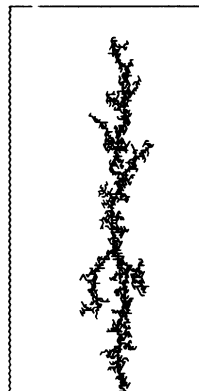We measure the fractal dimension of the clusters for two different values of the parameter β:

FIG. 7. A cluster started from a seed in the middle of the lattice.

$$D_F = 1.51 \pm 0.03 \; , \quad \beta = 0.001 \; , \tag{4}$$

$$D_F = 1.67 \pm 0.03 \; , \quad \beta = 0.5 \; . \tag{5}$$

However, these values are only indicative and we do not perform the analysis over the full range of the β values. This is because with such seed geometry it is impossible to define which part of the structure is really frozen, in the sense that it is asymptotically grown. In addition also the mass-gyration radius relation is clearly inappropriate because the shape does not have a circular symmetry. Nevertheless, the values obtained are very close to those measured with other seed geometries.

B. Seed on the fixed boundary side

In this scheme we used two types of seed. First, one side entirely made of broken bonds, secondly one broken bond at the center of the side. In both cases the pattern dynamics shows two growth phases. First a scaling regime, for crack heights smaller than the size of the base, followed by a steady-state regime in which the scaling properties are invariant along the growth direction (self-similar region).

The scaling regime is characterized by the competition between different trees of the growing pattern. In the steady state only one tree survives, screening the growth of the others. In this region the structures are statistically self-similar because, after the widths of patterns reach the maximum lattice size (the basis size), the structures have a single diverging length. The same result has been found by Evertsz [15] for DBM clusters grown in cylindrical geometry. We focus our attention on the upper square region of the cluster (steady-state zone [15]) where the fractal behavior does not depend on the height and the seed shape. In particular, we choose a region at height greater than L (usually $\frac{3}{2}L$) and at least at $\frac{1}{2}L$ from the tip of the structure. It is possible to show that in this region the pattern is statistically self-similar and asymptotically frozen.

Also in this case the structure is highly ramified and shows that the tip-splitting phenomenon is responsible for the pattern branching. In addition, the surviving tree of the steady state has the same features as the main branch of the simulations with a central seed. These results suggest that the steady-state regime is independent of the geometry of the starting seed.

We generate eight realizations for each value of the ratio β/α and the parameter η. We have determined the box-counting dimensions of a square section of the cluster suitably far from the boundaries. This is actually done by covering the region with boxes of sizes $l = 2^0, \ldots, 2^k$, where $k = \log L / \log 2$. The dimensions are obtained from the log-log plots, as shown in Fig. 8 for $\eta = 1$ and $\beta = 0$. Clearly the exponents are the quenched mean values of the slopes averaged over the number of realizations. The results are reported in Tables I–III.

In Table I we report the fractal dimension for different values of the parameter β. The most relevant result is the continuous dependence of the fractal dimension D_F on the value of β. This result does not agree with the conclusion, stated in Ref. [8], that the model shows two
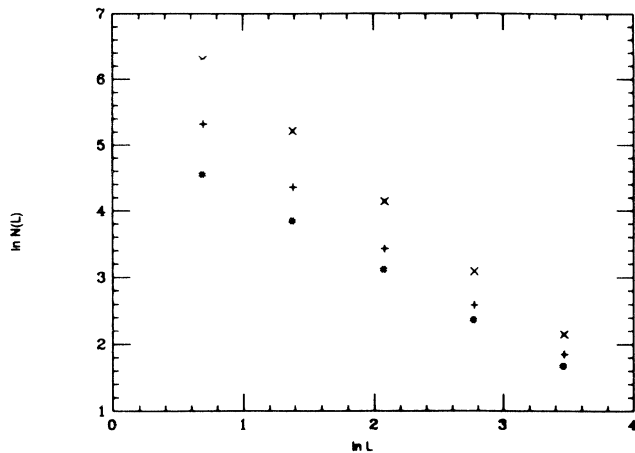

FIG. 8. Dependence of the number of full boxes $N(L)$ on the box size L for the cluster (top), the backbone (middle), and the chemical distance (bottom) for a typical realization of size 128×336.

universality classes, respectively, for $\beta = 0$ and $\beta \neq 0$. Actually, our results show very clearly that the fractal dimension changes continuously with the ratio (β/α), reaching an asymptotic value for $\beta/\alpha \rightarrow 0$. This result is supported also by the value of the fractal dimension of the cluster's backbone. In fact, also in this case the value of the exponent depends continuously upon the value of β. Moreover, there is not a clear distinction between structures with $\beta = 0$ and $\beta \neq 0$ but very small. It is important to notice that the value of D_B is close to the value of the fractal dimension of the whole clusters. Loops then play a major role in the pattern formation of this model. This is not surprising; in the Born model the possibility to form closed loops (which does not exist in DBM) makes the backbone properties closely related to those of the whole structure.

The results obtained for the chemical distance are very different. In this case the exponent D_C governing the scaling behavior of the minimum path length between two points takes on its one-dimensional value, $D_C = 1$, for all the values of the parameter β. Only for $\beta = 0$ does the value of D_C seem to be appreciably greater than 1. However, for larger sizes of the lattice (see Table II) the value is lower, leading to the conclusion that this anomaly is a

TABLE I. Values of fractal dimensions for $\eta = 1$ and several values of the ratio β/α. The cluster size is 64×168.

β	Simulations with $\eta = 1$ and $\alpha = 1$		
	D_F	D_B	D_C
0	1.52±0.04	1.41±0.04	1.09±0.03
0.001	1.55±0.04	1.42±0.04	1.03±0.03
0.01	1.61±0.04	1.47±0.04	1.01±0.02
0.05	1.63±0.04	1.53±0.04	1.01±0.03
0.1	1.68±0.03	1.58±0.04	1.01±0.02
0.5	1.70±0.03	1.59±0.04	1.05±0.03
5	1.74±0.03	1.62±0.03	1.03±0.03

TABLE II. Values of fractal dimensions for $\eta=1$, $\alpha=1$, $\beta=0$, and cluster size 128×336.

	Simulations with $\eta=1$, $\alpha=1$, $\beta=0$	
D_F	D_B	D_C
1.50 ± 0.03	1.28 ± 0.03	1.04 ± 0.02

TABLE III. Values of fractal dimensions for $\eta\neq1$. The cluster size is 64×168.

	Simulations with $\alpha=1$, $\beta=0$			
	$\eta=0.5$	$\eta=1$	$\eta=1.5$	$\eta=2$
D_F	1.85 ± 0.05	1.52 ± 0.04	1.35 ± 0.04	1.28 ± 0.03

finite size effect. The fact that D_C is equal to 1, independently of the internal parameters of the model, seems to be a common characteristic of fractal growth phenomena. In fact, the same result was found for DLA [17], where it suggests the absence of an upper critical dimension. In this sense, it should be important to test our results also for values of the Euclidean dimension greater than 2.

For the particular value $\beta=0$, we perform simulations with $\eta\neq1$ and for larger lattice sizes in order to test the convergency of the results. With respect to the parameter η the behavior is the usual one, found also for the DBM. For $\eta>1$ the screening effects of Eq. (1) are enhanced and the fractal dimension decreases for increasing value of η. The opposite phenomenon occurs for $\eta<1$ (see Table III). In Table II we report the values obtained for the exponents D_F, D_B, and D_C for clusters generated with $\beta=0$ and lattice size 128×336. While the fractal dimension of the whole cluster is stable with respect to the increasing lattice size, the value of D_B is appreciably changing. This calls for larger simulations in order to reduce finite size effects.

In summary , we have performed computer simulations of the Born model under uniaxial tension. We have obtained "directed" crack patterns with a well-defined growth direction that seem to be a realistic description of some kinds of experimental fractures. We investigate a wide range of the internal parameters of the model, and by developing an algorithm based on the topological properties of the clusters, we are able to isolate the backbone and the chemical distance of the generated clusters. With a box-counting procedure, we find the scaling behavior as a function of the internal parameters and boundary conditions. We find a continuous dependence of the fractal dimension on the parameter β that modulates the noncentral-force contribution in the elastic energy of the model. On the contrary, for the chemical distance, we have the same scaling exponent $D_C=1$ for every value of the internal parameters, suggesting that this is a common feature of fractal growth processes.

[1] Statistical Models for the Fracture of Disordered Media, edited by H. J. Herrmann and S. Roux (Elsevier, Amsterdam, 1990).

[2] T. Vicsek, Fractal Growth Phenomena (World Scientific, Singapore, 1992).

[3] H. J. Herrmann, Phys. Scr. T38, 13 (1991).

[4] L. Niemeyer, L. Pietronero, and H. J. Wiesmann, Phys. Rev. Lett. 52, 1033 (1984).

[5] T. A. Witten and L. M. Sander, Phys. Rev. Lett. 47, 1400 (1981).

[6] In this respect the algorithm developed recently by P. Ossadnik in close analogy to DLA seems to be very important, P. Ossadnik, HLRZ Report No. 106/92, 1993 (unpublished).

[7] E. Louis and F. Guinea, Europhys. Lett. 3, 871 (1987).

[8] H. Yan, G. Li, and L. M. Sander, Europhys. Lett. 10, 7 (1989).

[9] P. N. Sen and M. F. Thorpe, Phys. Rev. B 15, 4030 (1977).

[10] S. Feng and P. N. Sen, Phys. Rev. Lett. 52, 216 (1984).

[11] P. Meakin, G. Li, L. M. Sander, E. Louis, and F. Guinea, J. Phys. A 22, 1393 (1989).

[12] V. K. Horváth and H. J. Herrmann, Chaos Solitons Fractals 1, 395 (1991).

[13] L. Pietronero, A. Erzan, and C. Evertsz, Phys. Rev. Lett. 61, 861 (1988).

[14] L. Pietronero, A. Erzan, and C. Evertsz, Physica A 151, 207 (1987).

[15] C. Evertsz, Phys. Rev. A 41, 1830 (1990).

[16] L. D. Landau and E. M. Lifšits, Elasticity (Pergamon, New York, 1960).

[17] P. Meakin, I. Majid, S. Havlin, and H. E. Stanley, J. Phys. A 17, L975 (1984).